

Determination of the incommensurately modulated structure of Mo_8O_{23} by means of single-crystal X-ray diffraction

This article has been downloaded from IOPscience. Please scroll down to see the full text article.

1990 J. Phys.: Condens. Matter 2 45

(<http://iopscience.iop.org/0953-8984/2/1/003>)

View [the table of contents for this issue](#), or go to the [journal homepage](#) for more

Download details:

IP Address: 171.66.16.96

The article was downloaded on 10/05/2010 at 21:21

Please note that [terms and conditions apply](#).

Determination of the incommensurately modulated structure of Mo_8O_{23} by means of single-crystal x-ray diffraction

Arjan J H Komdeur, Jan L de Boer and Sander van Smaalen[†]
Laboratory of Inorganic Chemistry, Materials Science Centre, University of Groningen,
Nijenborgh 16, NL 9747 AG Groningen, The Netherlands

Received 13 July 1989

Abstract. Mo_8O_{23} is incommensurately modulated between the temperatures 285 K and 360 K. In this article results are presented on the determination of the structure of this compound at 298 K. The monoclinic cell parameters are determined to be $a = 13.382(1)$ Å, $b = 4.0519(6)$ Å, $c = 16.877(2)$ Å and $\beta = 106.197(3)^\circ$. The space group of the average structure is found to be $P2_1/c$, in accordance with previous studies. The observed satellite reflections can be indexed using a single modulation wavevector, which has components (0.188, 0.5, 0.133). The superspace group characterising the symmetry of the incommensurately modulated structure is $B_{11}^{P2_1/c}$. Refinement on 6270 main reflections and 1940 satellites, with $I > 2.5\sigma(I)$, gave convergence to a weighted R -factor of 0.029, with partial R -factors of 0.024 for main reflections and 0.095 for satellite reflections. The modulation is interpreted as a combination of rotations and distortions of the MoO_6 octahedra.

1. Introduction

Octomolybdenum tricosaoxide is one of several phases occurring in the molybdenum-oxygen phase diagram. The structures of these phases were first studied by Magnéli, who introduced the concept of homologous series to designate the $\text{Mo}_n\text{O}_{3n-m}$, $m = 0, 1, 2$ compounds (Magnéli 1953). Mo_8O_{23} belongs to the homologous series with $m = 1$. Later, more accurate refinements were presented by Kihlborg (1963a).

Recently, the molybdenum oxides were studied by Sato and coworkers (Sato *et al* 1984, 1986, 1987, Fujishita *et al* 1987). They focused on the physical properties, but also presented new structural studies. An interesting new feature was that the structures of several of these compounds are superstructures of the structures proposed by Magnéli, or are even incommensurately modulated.

The structures of the $\text{Mo}_n\text{O}_{3n-1}$ homologous series are related to the cubic ReO_3 -type structure. The latter compound consists of corner-linked ReO_6 octahedra, the cubic axes being equal to the vectors between opposite oxygen atoms in one octahedron. This same building principle applies to the $\text{Mo}_n\text{O}_{3n-1}$ compounds. Rows of n corner-sharing

[†] Author to whom correspondence should be addressed.

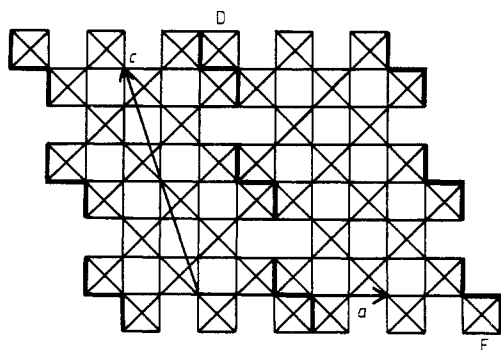


Figure 1. Projection of the structure of $\text{Mo}_n\text{O}_{3n-1}$ along b , for $n = 8$. The edges common to two octahedra are indicated by thick lines, which together form a shear plane. Going from D to E, n corner-sharing octahedra are found, representing the 'width' of the slab with ReO_3 structure.

MoO_6 octahedra are separated by so-called crystal shear planes, which accommodate the oxygen deficiency by edge sharing of the octahedra (figure 1).

Octomolybdenum tricosaoxide has two phase transitions. Above $T_{c1} = 360$ K the structure is monoclinic, with space group $P2/c$ and lattice parameters at $T = 370$ K of $a = 13.384(3)$ Å, $b = 4.0616(5)$ Å, $c = 16.883(3)$ Å and $\beta = 106.27(2)^\circ$ (Fujishita *et al* 1987). The structure at this temperature was found to be equal to the one previously given as the room temperature structure (Fujishita *et al* 1987, Magnéli 1948, Kihlberg 1963*b*). It represents, however, only the average structure at room temperature, whereas it is the true structure at 370 K. Below $T_{c2} = 285$ K the structure is a simple superstructure of the high-temperature structure, with a doubled b -axis. The superstructure formation was interpreted as a rotation of the MoO_6 octahedra (Sato *et al* 1986, Fujishita *et al* 1987). Between T_{c1} and T_{c2} the structure is incommensurately modulated, with a modulation wave vector $\mathbf{q} = (\alpha, 0.5, \gamma)$ (Sato *et al* 1986, Fujishita *et al* 1987), for which they determined the values $\alpha = 0.195$ and $\gamma = 0.120$.

In this paper we report on the determination of the structure of the incommensurate phase, as done by means of single-crystal, x-ray diffraction at room temperature.

2. Experimental details

Single-crystal x-ray diffraction experiments were performed on an ENRAF-NONIUS CAD4F four-circle diffractometer, using $\text{Mo K}\alpha$ radiation ($\lambda = 0.71073$ Å) and a graphite monochromator. Two crystals were used. The smaller (crystal I) was a platelet of thickness 0.094 mm along b and irregular shaped in the ac plane with approximate dimensions 0.2 mm \times 0.2 mm. Its volume was 0.0028 mm³. The larger crystal (crystal II) was also an irregular shaped platelet, but now of approximate dimensions 0.4 mm \times 0.4 mm, thickness 0.20 mm and volume 0.031 mm³. Optimisation of the positions of twenty first-order satellites of crystal I allowed the determination of the modulation wave vector as $\mathbf{q} = (0.188, 0.5, 0.133)$. The unit cell is obtained from the positions of four alternative settings of 22 reflections with θ between 30° and 32°. It was found to be monoclinic within experimental accuracy. The lattice parameters are, $a = 13.382(1)$ Å, $b = 4.0519(6)$ Å, $c = 16.877(2)$ Å and $\beta = 106.197(3)^\circ$. They compare well with the values reported previously (Magnéli 1948, Fujishita *et al* 1987).

In order to minimise absorption and extinction, crystal I was used for measuring the main reflections. Intensities of a total of 14 439 reflection positions were measured. The angle θ varied between 1.26° and 45°. Minimum and maximum reflection indices were:

h from -26 to 25 , k from -8 to 8 and l from 0 to 33 . Three reference reflections, $(4, 0, 6)$, $(-4, 2, 1)$ and $(-1, 2, 4)$, were recorded every 2 hours and were used to calculate a correction for drift in intensity of the principal beam. The average variation was 0.8% . After correction for the Lorentz and polarisation effects and for absorption ($\mu = 5.51 \text{ mm}^{-1}$), equivalent reflections were averaged in Laue symmetry $2/m$. The internal consistency $R_I = (\Sigma\Delta I)/(\Sigma I) = 0.0164$ proved this to be the correct point group. Removal of the absorption correction (minimum and maximum values 1.63 and 2.28 , respectively) did not change this value. Analysis of the systematic extinctions pointed to the presence of a c -glide, in accordance with previous studies (Magnéli 1948, Fujishita *et al* 1987). A total of 7222 unique reflections were obtained, of which 6270 with $I > 2.5\sigma(I)$ were used in the refinements.

Crystal II was used to measure the much weaker satellite reflections. A total of 21 707 first-order satellites in the θ range from 2.54° to 44.88° were measured. Minimum and maximum reflection indices were: h from -25 to 24 , k from -13 to 13 and l from 0 to 31 . Both $m = -1$ and $m = 1$ satellites were measured. Correction for drift in the intensity of the primary beam was now applied using the reference reflections $(4, 0, 6)$, $(-4, 4, 1)$ and $(-1, 4, 4)$, measured every 2 hours. Average variation was 0.8% . After correction for the Lorentz and polarisation effects and for absorption, the intensities were averaged in Laue symmetry $2/m$. Despite the larger absorption (minimum and maximum values 2.71 and 5.32 , respectively) the internal consistency did not depend on whether absorption correction was applied or not. Excluding 'less than's' (reflections with $I < 2.5\sigma(I)$) $R_I = 0.068$ is obtained. This is not as good as for the main reflections, which can be attributed to the larger fraction of reflections being just above the 'less-than' threshold. Compare the values for $R_\sigma = (\Sigma\sigma(I))/(\Sigma I)$ which is 0.029 for the main reflections, but only 0.116 for the satellites. A total of 10 855 unique satellite reflections were obtained, of which 1940 with $I > 2.5\sigma(I)$ were used in the refinements.

The analysis requires that the relative scale between the main reflections and the satellites is known. To this end 496 main reflections of intermediate intensity were measured on crystal II. By excluding strong reflections, extinction was avoided as much as possible. The relative scale between reflections from crystal I and reflections from crystal II was then calculated as the average ratio of corresponding reflections from the two crystals. A value of $11.2(8)$ for the ratio of crystal II to crystal I was obtained. All intensities of crystal I were multiplied by this factor. It turned out that application of the absorption correction improved the accuracy from 10% without correction to 7% with absorption correction. Apparently, the two equivalent reflections in one crystal did have about the same path length through the crystal, whereas the path lengths of the same reflection in the two different crystals were not completely correlated. It proves the necessity of the absorption correction, despite its null-effect on R_I .

3. Symmetry

In the previous section it was already revealed that the symmetry of the average structure is given by the space group $P2/c$, in accordance with previous studies (Magnéli 1948, Kihlberg 1963b, Fujishita *et al* 1987).

To be able to describe the symmetry and structure of the incommensurately modulated phase, the theory of superspace groups is applied (De Wolff *et al* 1981). Reflections are indexed with four integers as

$$S = ha^* + kb^* + lc^* + mq.$$

The three reciprocal basis vectors together with the vector q are then identified with four

reciprocal basis vectors in a four-dimensional space. This makes it possible to describe the symmetry by a four dimensional space group (De Wolff *et al* 1981). The analysis of the diffraction symmetry and the extinction conditions is analogous to that for ordinary crystals. To facilitate the analysis of the extinction conditions it is useful to transform to a larger basic structure unit cell, such that the commensurate components of the modulation wavevector disappear (De Wolff *et al* 1981). The transformation involved is a doubling of the b axis, i.e. $A = a$, $B = 2b$ and $C = c$. The entirely incommensurate wavevector is $q_i = (0.188, 0, 0.133)$. The transformed indices are given by (H, K, L, M) , with $H = h$, $K = 2k + m$, $L = l$ and $M = m$.

The point symmetry of the diffraction pattern including the satellite reflections is $2/m$ (§ 2). With respect to the transformed indices (H, K, L, M) the following systematic extinctions are observed:

$K + M = \text{odd}$ is absent for the (H, K, L, M) reflections

$L = \text{odd}$ is absent for the $(H, 0, L, M)$ reflections.

The first condition reflects the presence of the centring translation $ct = (0, \frac{1}{2}, 0, \frac{1}{2})$, and is a result of the above-mentioned transformation. The second condition represents a c -glide perpendicular to b . At this stage, however, it is not possible to determine the fourth translational component of this operator. According to the first extinction condition, all first-order satellites of the type $(H, 0, L, M)$ are absent. The second condition can thus be written as $L = \text{odd}$ is absent or as $L + M = \text{odd}$ is absent. Only the observation of second-order satellites could distinguish between these two conditions. As only first-order satellites were observed, both possibilities remain. They correspond to the $(3 + 1)$ -dimensional superspace groups $B_{11}^{P2/c}$ and $B_{1s}^{P2/c}$.[†] The refinements will show the correct symmetry to be $B_{11}^{P2/c}$.

4. Refinement of the average structure

Refinements of the average structure were performed using the 6270 main reflections with $I > 2.5\sigma(I)$. Atomic scattering factors for Mo^{6+} and O^{1-} , including dispersion corrections, were taken from *International Tables* vol IV (1974). Starting values for the parameters were the coordinates given by Fujishita *et al* (1987). With the XTAL program package (Hall and Stewart 1987) reliability factors $R_F = (\sum |F_0| - |F_c|) / (\sum |F_0|) = 0.022$ and $wR_{F2} = \{[\sum w(|F_0| - |F_c|)^2] / (\sum w|F_0|^2)\}^{1/2} = 0.026$ were obtained, using unit weights. The same calculation, but performed with the program REMOS (Yamamoto 1985) leads to somewhat larger R -factors, $R_F = 0.023$ and $wR_{F2} = 0.034$, probably due to a different treatment of the correction for secondary extinction. For comparison with the refinement of the modulated structure, the calculations were repeated with weights equal to $1/\sigma^2(F)$. Slightly lower R -factors were obtained: $R_F = 0.022$ and $wR_{F2} = 0.024$. The result of the refinements does not differ significantly from the coordinates given by Fujishita *et al* (1987), thus proving the average structure given by Magnéli (1948) and Kihlberg (1963b) to be correct. As the coordinates do not differ appreciably from the average position coordinates obtained in the refinement of the

[†] Both superspace groups are in fact equivalent. If one of them applies to a structure with modulation wavevector q , then the other describes the same structure, but with the alternative modulation wavevector $q' = a^* + b^* + c^* - q$. The ambiguity referred to here is that one cannot distinguish between both superspace groups, even when using a single modulation wavevector.

modulated structure, we omit them here. They can be obtained from the authors on request.

5. The modulated structure

The presence of satellite reflections at positions $q = (0.188, 0.5, 0.133)$ from the main reflections shows the structure to be incommensurately modulated. Both the low-temperature, commensurately modulated structure (Fujishita *et al* 1987) and the average structure itself suggest that the modulation will be of the displacive type.

Only first-order satellites could be observed. This means that only the first harmonic in the Fourier expansion of the modulation function can be determined (Van der Aalst 1976). For atom μ on average position r_0^μ , this displacive modulation is given by

$$u_\alpha^\mu(\bar{x}_4) = A_\alpha^\mu \cos(2\pi\bar{x}_4) + B_\alpha^\mu \sin(2\pi\bar{x}_4) \quad \alpha = x, y, z \quad (1)$$

with $\bar{x}_4 = q \cdot r_0^\mu$, and the actual, unit-cell-dependent, position

$$r^\mu = r_0^\mu + u^\mu(\bar{x}_4). \quad (2)$$

For each atom on a general position in the average structure unit cell, three average position parameters and six modulation parameters were included in the refinement. A possible modulation of the temperature parameters is not taken into account. Now there are six independent temperature parameters per atom, for anisotropic temperature factors.

There is only one atom on a special position of the average structure: O1 on $(0, 0.25, 0)$ on an inversion centre (coordinates with respect to the A, B, C unit cell). Denote a symmetry operator of the superspace group by $(R \varepsilon | \tau_1, \tau_2, \tau_3, \tau_4)$, with R the three-dimensional part of the point group operator, ε its fourth element and τ_1, \dots, τ_4 the translational components along the four axes in superspace. Then, symmetry restrictions on the modulation functions are obtained from $(i \bar{1} | 0, \frac{1}{2}, 0, \frac{1}{2}) u^\mu(\bar{x}_4) = u^\mu(\bar{x}_4)$, which leads to the B_α^μ parameters being equal to zero for O1. The anisotropic temperature tensor remains unrestricted.

Two strategies were employed to determine the modulation function. At first, the low temperature superstructure as determined by Fujishita *et al* (1987) at $T = 100$ K was used to obtain starting values for the position parameters. For each pair of atoms at approximately y and $y + \frac{1}{2}$, the position was written as an average value plus or minus a deviation, for the atoms at y and $y + \frac{1}{2}$, respectively. This deviation then gives the amplitude of the modulation function. To obtain an estimate for the amplitudes in the incommensurately modulated phase these values were multiplied by the square root of the ratio of the intensities of a satellite at the two temperatures, which is a factor of 0.3 (Sato *et al* 1986). Only the largest amplitudes were used for the starting model. Refinement of all independent parameters in symmetry $B_{11}^{P2/c}$ with the program REMOS (Yamamoto 1985) converged smoothly to a reliability factor $wR_{F2} = 0.035$ (main reflections: $wR_{F2} = 0.034$; satellites: $wR_{F2} = 0.181$) for 6270 main reflections and 1940 satellites. Unit weights were used and corrections for dispersion effects and secondary extinction were included.

In a second approach all modulation parameters were initially set to zero. Within error boundaries refinement lead to the same structural model as the former, but now with $wR_{F2} = 0.187$ for the satellite reflections. Changing signs of one or several of the largest parameters gave, after further refinement, the same model or one with a higher

Table 1. Reliability factors for the final structure model. The values with unit weights are calculated for the structure model obtained from the refinement using weights equal to $1/\sigma^2(F)$.

	$w = 1/\sigma^2(F)$		Unit weights
	R_F	wR_{F2}	wR_{F2}
Main reflections	0.023	0.024	0.034
Satellites	0.140	0.095	0.184
All reflections	0.027	0.029	0.035

Table 2. Average position coordinates and the modulation parameters for the result of the refinement of the modulated structure. Values refer to the transformed unit cell: $A = 13.382 \text{ \AA}$, $B = 8.104 \text{ \AA}$, $C = 16.877 \text{ \AA}$ and $\beta = 106.2^\circ$. They are multiplied by 10^4 . Standard deviations in the last digit are given in parentheses.

Atom	x_0	y_0	z_0	A_x	B_x	A_y	B_y	A_z	B_z
Mo(1)	639.9(1)	2925.4(2)	4166.2(1)	12.8(4)	2.5(6)	13(1)	3.2(6)	-4.6(3)	2.1(5)
Mo(2)	1850.9(1)	2066.8(2)	2457.5(1)	6.9(6)	-3.0(3)	-13.1(9)	6(1)	-17.5(5)	-0.7(3)
Mo(3)	3149.7(9)	2948.9(2)	790.7(1)	1.2(4)	-0.1(3)	8.3(8)	5.3(7)	-6.0(4)	-3.0(3)
Mo(4)	4465.9(1)	2041.7(2)	4020.3(1)	-0.5(2)	0.6(2)	-1.3(4)	0.2(5)	-1.9(2)	0.6(2)
O(1)	0	0.25	0	8(6)		249(9)		-35(5)	
O(2)	657(1)	9(2)	4163(1)	-81(3)	-57(5)	-2(8)	-29(5)	47(2)	62(4)
O(3)	1918(1)	4977(2)	2458(1)	-27(4)	72(3)	5(7)	-52(7)	102(3)	-7(3)
O(4)	3195(1)	43(2)	771(1)	-25(5)	-42(4)	3(7)	-26(7)	30(5)	19(4)
O(5)	4476(1)	4946(2)	4071(1)	4(3)	-4(3)	-2(5)	-2(6)	33(3)	9(3)
O(6)	644(1)	2473(2)	1646(1)	-43(5)	-7(2)	55(12)	29(5)	-62(4)	-16(2)
O(7)	1293(1)	2468(2)	3306(1)	19(4)	15(4)	-151(8)	-86(8)	-12(3)	13(3)
O(8)	1992(1)	2473(2)	4958(1)	-1(4)	-10(4)	0(9)	32(9)	-44(3)	-42(3)
O(9)	2609(1)	2570(2)	1635(1)	-19(3)	-19(4)	120(7)	-23(7)	-10(3)	3(3)
O(10)	3263(1)	2453(2)	3277(1)	-31(4)	9(4)	46(8)	3(8)	12(3)	32(3)
O(11)	4104(1)	2506(2)	45(1)	17(3)	3(3)	-57(6)	-11(5)	10(3)	9(2)
O(12)	4572(1)	2453(2)	1538(1)	5(3)	-8(4)	61(6)	8(6)	-1(2)	2(2)

R -factor, thus indicating that the structure model originally found gives the true minimum in wR_{F2} .

The partial R -factor for the satellite reflections is rather high. This may be attributed to the fact that many satellites are just above the 'less than' threshold of $2.5\sigma(I)$. Therefore, new refinements were performed with weights equal to $1/\sigma^2(F)$, where $\sigma(F)$ is the standard deviation in the structure factor corresponding to the statistical error in the measured intensities. The resulting reliability factors are summarised in table 1. Note that the R -factor with unit weights as calculated for the structure obtained by refinement with weights equal to $1/\sigma^2(F)$ is about the same as in the refinement using unit weights, whereas the $1/\sigma^2(F)$ weights lead to a considerably lower R -factor. Furthermore, it is found that the values of the parameters are almost the same in both refinements. This is another indication for the correctness of the model found. The position parameters of the final model are given in table 2, anisotropic temperature factors are given in table 3.

Table 3. Anisotropic temperature factors of the final model for the modulated structure. All values are multiplied by 10^4 ; standard deviations in the last digit are given in parentheses. The values refer to the transformed unit cell: $A = 13.382 \text{ \AA}$, $B = 8.104 \text{ \AA}$, $C = 16.877 \text{ \AA}$ and $\beta = 106.2^\circ$. The temperature factor for the structure factor is of the form

$$\exp[-(h^2\beta_{11} + k^2\beta_{22} + l^2\beta_{33} + 2hk\beta_{12} + 2kl\beta_{23} + 2hl\beta_{13})].$$

Atom	β_{11}	β_{22}	β_{33}	β_{23}	β_{31}	β_{12}
Mo(1)	5.51(5)	16.0(1)	3.18(3)	-0.03(5)	1.38(3)	-0.15(7)
Mo(2)	4.89(4)	16.7(1)	2.74(3)	-0.04(5)	1.19(3)	-0.21(6)
Mo(3)	4.42(4)	16.3(1)	3.42(3)	-0.06(5)	1.36(3)	-0.01(6)
Mo(4)	4.29(4)	16.4(1)	3.04(3)	-0.64(5)	0.60(2)	-0.58(6)
O(1)	10.6(8)	37(5)	3.5(5)	7(1)	4.5(5)	0(2)
O(2)	16(1)	20(2)	12.5(7)	2.1(8)	5.8(6)	-2(1)
O(3)	15.1(8)	19(2)	7.6(7)	-0.8(9)	4.3(6)	4(1)
O(4)	12.7(8)	17(2)	17.0(6)	0.8(7)	6.0(5)	-1.1(8)
O(5)	14.7(6)	22(1)	9.5(5)	-1.7(6)	3.4(4)	-0.9(7)
O(6)	5.9(6)	51(2)	1.7(5)	4.8(9)	-2.8(5)	2.9(9)
O(7)	10.6(6)	74(4)	4.5(4)	-3.0(9)	4.7(4)	5(1)
O(8)	7.6(6)	51(2)	2.7(5)	2.5(8)	-1.5(4)	1.8(7)
O(9)	10.9(6)	59(2)	5.5(4)	3.8(7)	4.5(4)	3.5(9)
O(10)	6.8(6)	45(2)	5.1(4)	-0.5(7)	-0.6(4)	0.6(8)
O(11)	6.7(5)	36(2)	3.5(3)	1.1(5)	1.7(3)	2.0(7)
O(12)	6.4(5)	43(2)	4.3(3)	0.3(6)	1.7(3)	1.4(7)

To test the symmetry, refinements were also performed using the superspace group $B_{15}^{P2/c}$. An overall R -factor of $wR_{F2} = 0.045$, with partial R -factors 0.040 (main reflections) and 0.482 (satellites) was obtained. This is much higher than in the superspace group $B_{11}^{P2/c}$, thus proving the latter to be the correct superspace group describing the symmetry of this phase.

6. Discussion

The distortion of the low-temperature superstructure was interpreted as mainly inhomogeneous rotations of the MoO_6 octahedra around a vector parallel to q_1 . This should then be accompanied by expansion and contraction of the octahedra (Sato *et al* 1986).

From table 2 it is easy to calculate that the largest amplitudes along b occur on O(1), O(7) and O(9), ranging from 0.142 \AA to 0.070 \AA . The largest amplitudes in the (a, c) plane are present on the atoms O(2) and O(3), being 0.164 \AA and 0.151 \AA , respectively. From figure 2 it follows that this is exactly what is expected for a rotation of the octahedra. A rotation of all octahedra is not possible, due to the edge-sharing of several of them. This is found in the structure model where not only O(6), O(8) and O(10), but also O(5) and O(11) have small amplitudes.

Although the amplitudes of the individual atoms are in accordance with a model of rotating octahedra, this is not sufficient to conclude on such a distortion. In order to obtain a more detailed picture of the modulation, the interatomic distances are studied as a function of the phase of the modulation wave.

In figure 3(a) the distances are plotted between oxygen atoms at $y \approx 0.5$ of a series of octahedra on a line perpendicular to q_1 . Because of the periodicity of the modulation

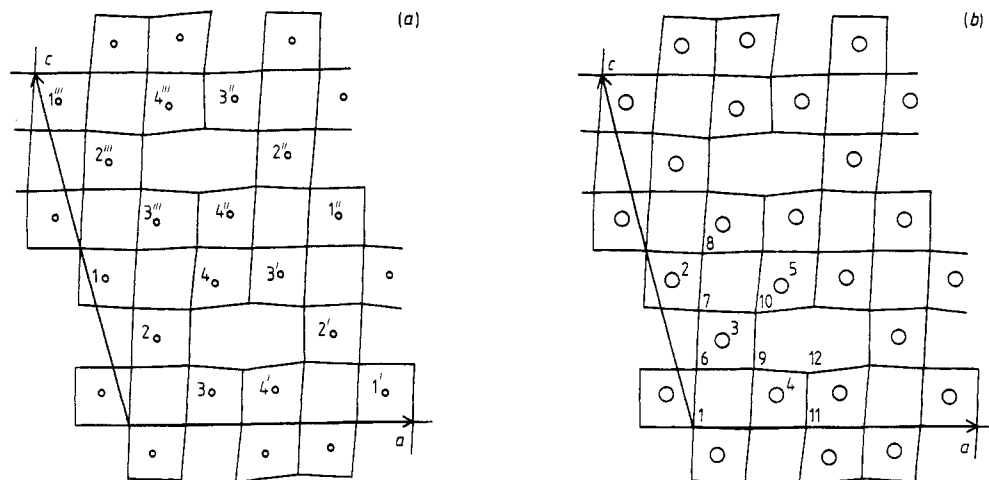


Figure 2. (a) Projection of one unit cell of the average structure of Mo_8O_{23} . The numbers 1 through 4 indicate the corresponding molybdenum atoms in table 2. Single primed numbered atoms are obtained through the application of the two-fold axis at $(0.5, y, 0.25)$ to the coordinates in table 2; double-primed numbers are obtained with the inversion centre at $(0.5, 0.5, 0.5)$; triple-primed numbers follow from the c -glide at $(x, 0.5, z)$ applied to the coordinates in table 2. (b) The same projection as in (a) but now with the oxygen atoms indicated by a number corresponding to the same atom in table 2.

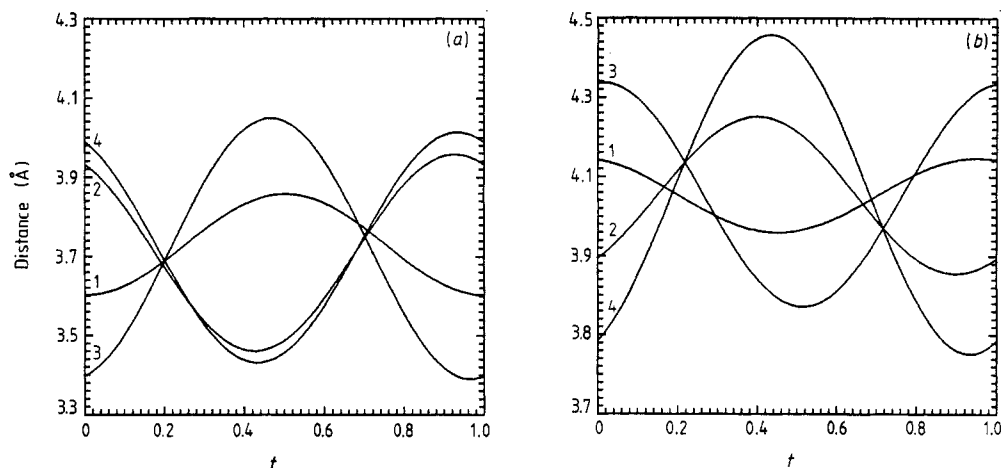


Figure 3. (a) Interatomic distances between top-oxygen atoms ($y \approx 0.5$) of a series of neighbouring octahedra in a line perpendicular to q_1 . The distance is plotted as a function of the phase t of the modulation wave, where the displacements of the individual atoms are given by $u^\mu(\mathbf{q} \cdot \mathbf{r}_\mu^\dagger + t)$. The four lines correspond to the following distances (see figure 2): 1, $(m_y \bar{1}|0, 1, -0.5, 0)\text{O}(5)$ with $(E|0, 0.5, 0, 0.5)\text{O}(4)$; 2, $(E|0, 0.5, 0, 0.5)\text{O}(4)$ with $\text{O}(3)$; 3, $\text{O}(3)$ with $(E|0, 0.5, 0, 0.5)\text{O}(2)$; 4, $(E|0, 0.5, 0, 0.5)\text{O}(2)$ with $(i \bar{1}|0, 0.5, 1, 0.5)\text{O}(2)$. (b) Interatomic distances between an oxygen atom on $(x, y = 0.25, z)$ and one translated over $(E|0, 0.5, 0, 0.5)$, for the atoms connecting the octahedra used in figure 3(a). The distances plotted are for the following atoms: 1, $\text{O}(11)$; 2, $\text{O}(9)$; 3, $\text{O}(7)$; 4, $(m_y \bar{1}|0, 0.5, 0.5, 0.5)\text{O}(1)$.

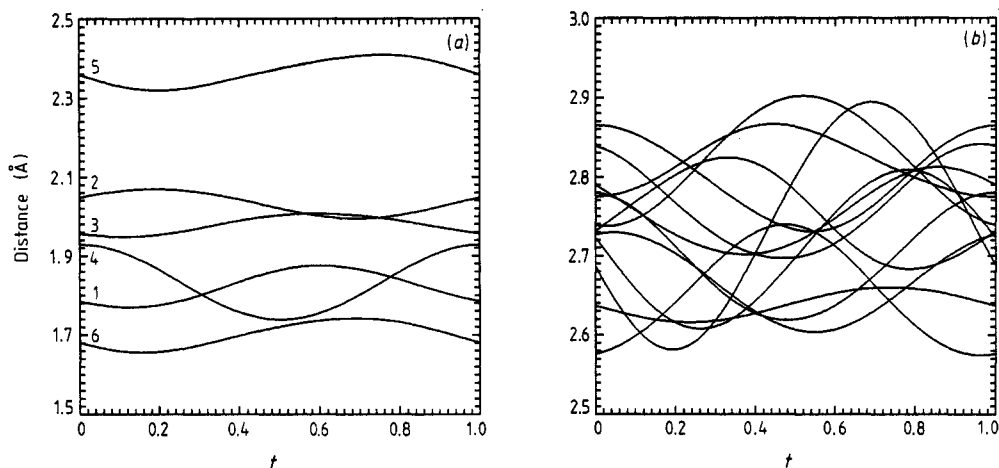


Figure 4. (a) Distances between Mo(2) and the six nearest-neighbour oxygen atoms, as a function of the phase of the modulation functions. The numbers correspond to the distance between Mo(2) and the following oxygen atoms: 1, O(7); 2, O(10); 3, O(9); 4, O(6); 5, O(3); 6, (E 1|0, -0.5, 0, 0.5)O(3). (b) The lengths of the twelve edges (oxygen-oxygen distances) of the octahedron around Mo(2).

functions, the values for t from 0 to 1 represent all interatomic distances occurring in the structure. From figure 3(a) one sees that distance 1 has the least variation, and is indeed a distance between atoms in edge-sharing octahedra. The variation in the distances 2 and 4 is in phase, but is almost 90° out of phase with distance 3, as one would expect for a rotation of octahedra. Comparison of figures 3(a) and 3(b) shows that when a top-top distance shortens, the corresponding distance along b elongates and vice versa. This is again in accordance with the picture of rotating octahedra. The maximum rotation can be estimated from these figures as half the maximum variation in plotted distances. A value of approximately 0.33 \AA is obtained for the octahedron around Mo(1).

To obtain an idea about the importance of the distortions of the octahedra, the Mo-O distances and O-O distances (edge lengths) within one octahedron are given in figure 4. The largest distortions are obtained for the octahedron around Mo(2), with maximum variation in the Mo-O distance of 0.19 \AA and in the O-O distance of 0.31 \AA . The corresponding values for the octahedron around Mo(1) are 0.18 \AA and 0.24 \AA , respectively. The maximum values of the part of the displacements contributing to the distortion of the octahedra are then obtained as 0.16 \AA for oxygen and 0.03 \AA for molybdenum. Comparison of these values with the rotation amplitudes obtained from figure 3, shows that about $\frac{2}{3}$ of the magnitude of the displacements of the atoms can be attributed to a rotation of the MoO_6 octahedra and that about $\frac{1}{3}$ of the magnitude is connected with a distortion of the octahedra.

Acknowledgments

We are greatly indebted to Professor M Sato for making the crystals available to us. This work was supported in part by the EEC under contract No SC1-0032-c (CD). The

research of S van Smaalen has been made possible by financial support of the Royal Dutch Academy of Arts and Sciences (KNAW).

References

- De Wolff P M, Janssen T and Janner A 1981 *Acta Crystallogr. A* **37** 625–36
Fujishita H, Sato M, Sato S and Hoshino S 1987 *J. Solid State Chem.* **66** 40–6
Hall S R and Stewart J M (ed.) 1987 *XTAL2.2 User's Manual* Universities of Western Australia and Maryland
Kihlborg L 1963a *Ark. Kemi* **21** 471–95
—— 1963b *Ark. Kemi* **21** 461–9
Magnéli A 1948 *Acta Chem. Scand.* **2** 501–17
—— 1953 *Acta Crystallogr.* **6** 495–500
Sato M, Fujishita H, Sato S and Hoshino S 1986 *J. Phys. C: Solid State Phys.* **19** 3059–67
Sato M, Nakao K and Hoshino S 1984 *J. Phys. C: Solid State Phys.* **17** L817
Sato M, Onada M and Matsuda Y 1987 *J. Phys. C: Solid State Phys.* **20** 4763–71
Van der Aalst W, Den Hollander J, Peterse W J A M and De Wolff P M 1976 *Acta Crystallogr. B* **32** 47–58
Yamamoto A 1985 *REMOS 85* National Institute for Research in Inorganic Materials, Sakura-Mura, Niihari-Gun, Ibaraki 305, Japan